Characterization of Monoclonal Antibody Charge Variants under Near-Native Separation Conditions using Nanoflow Sheath Liquid Capillary Electrophoresis-Mass Spectrometry

Annika A.M. van der Zon[1,2,*], Alisa Höchsmann[3,4], Tijmen S. Bos[1,2], Christian Neusüß[3], Govert W. Somsen[2,5], Kevin Jooß[2,5], Rob Haselberg[2,5] and Andrea F.G. Gargano[1,2,*]

[1] University of Amsterdam, van 't Hoff Institute for Molecular Sciences, Analytical Chemistry Group, Science Park 904, 1098 XH Amsterdam, The Netherlands

[2] Centre of Analytical Sciences Amsterdam, Science Park 904, 1098 XH Amsterdam, The Netherlands

[3] Aalen University, Department of Chemistry, Beethovenstraße 1, 73430 Aalen, Germany

[4] Eberhard Karls University of Tübingen, Faculty of Science, 72074 Tübingen, Germany

[5] Vrije Universiteit Amsterdam, Department of Chemistry and Pharmaceutical Sciences, Amsterdam Institute of Molecular and Life Sciences, Division of BioAnalytical Chemistry, De Boelelaan 1085, 1081 HV Amsterdam, The Netherlands

[*] Correspondence: a.a.m.vanderzon@uva.nl and a.gargano@uva.nl

Highlights

- A CZE-UV/MS method to analyze the charge heterogeneity of intact mAbs was developed
- A static neutral HPMC coating was used in combination with volatile BGEs at pH 5.0
- The nanoCEasy interface was implemented to allow for MS coupling
- A useful tool for in-depth charge variants characterization of mAbs

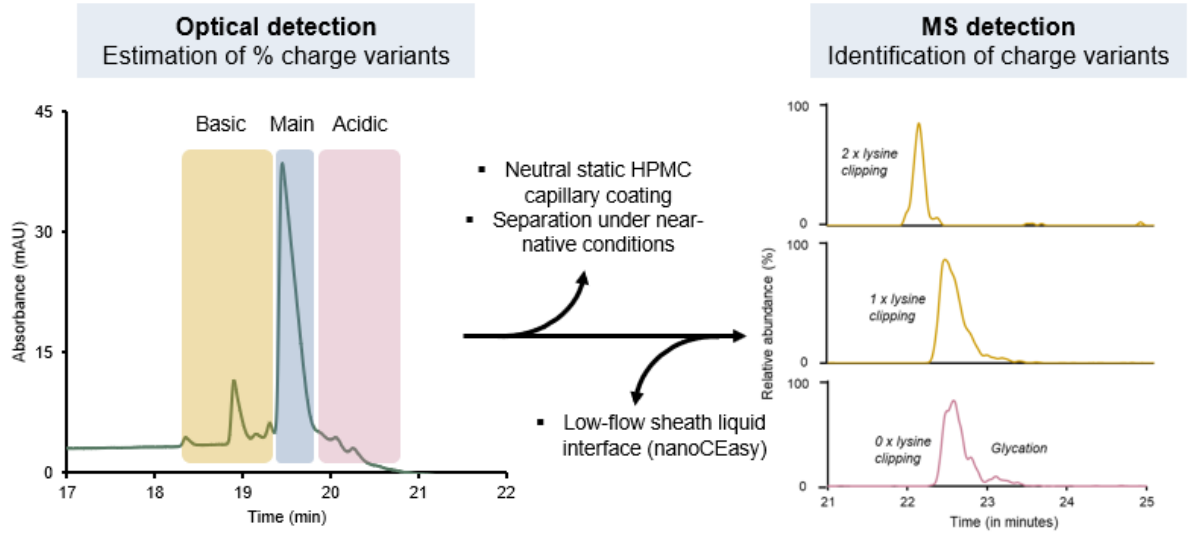

Graphical abstract: CZE-UV/MS analysis for the separation of charge variants of mAbs under near-native separation conditions

Abstract

Background: Monoclonal antibodies (mAbs) undergo multiple post-translational modifications (PTMs), *e.g.*, charge variants, oxidation, etc., during production and storage, necessitating evaluation of the resulting PTMs as critical quality attributes (CQA) for protein quality and safety. Charge variants PTMs can be separated using capillary zone electrophoresis (CZE). The CZE EACA method developed by He *et al.* (2011) with UV detection is applied routinely in the pharmaceutical industry for analyzing charge variants. However, the method cannot be directly hyphenated with mass spectrometry (MS), preventing direct identification of separated charge variants due to the non-volatile background electrolyte (BGE), which hinders reliable charge variant identification.

Results: This study presents a CZE-UV/MS method using a neutral static capillary coating of hydroxypropyl methylcellulose combined with a volatile BGE at pH 5.0 to allow MS-compatible mAb charge variant separations. The effect of several parameters, including pH and concentration of BGE, voltage, and injected mAb concentrations in terms of separation performance on a panel of mAbs was investigated. The final method was tested with mAbs of IgG subclasses (IgG_1 and IgG_4) with different pI (7.4-9.2), and degrees of heterogeneity. Basic and acidic variants were separated from the parent mAb using a BGE of 50 mM acetic acid adjusted at pH 5.0. A linear correlation in relative charge variant abundance was obtained between our method and the EACA method. CZE-MS coupling was done using the nanoCEasy, a low-flow sheath liquid interface, and allowed the identification and quantitation of various low-abundance variants (<10% relative abundance with respect to the main compound).

Significance: This method uses volatile buffers and operates at pH closer to non-denaturing conditions (pH 5.0), allowing for flexibility in hyphenation with MS. This method can be a useful tool for in-depth charge variants characterization of mAbs.

Keywords

Monoclonal antibodies, charge heterogeneity, capillary zone electrophoresis, mass spectrometry, hydroxypropyl methylcellulose, nanoCEasy

1. Introduction

Monoclonal antibodies (mAbs) are a fast-growing class of therapeutic agents used for the treatment of several major diseases [1]. mAbs are complex and heterogeneous proteins consisting of two light and two heavy oligopeptide chains connected via disulfide bridges. In addition, mAbs typically possess two or more glycosylation sites. During manufacturing and storage, mAbs can undergo multiple enzymatic and chemical post-translational modifications (PTMs). The presence or quantity of these modifications can impact the efficacy and safety of the biopharmaceutical product [2]. In this context, critical quality attributes (CQAs) are a set of carefully defined product characteristics that represent an important measure to ensure product quality. One of these CQAs is charge heterogeneity which encompasses both acidic proteoforms (originating from deamidation, sialylation, and glycation), as well as basic proteoforms (*e.g.* lysine truncation, N-terminal glutamine/pyroglutamate conversion, and succinimide formation) [3,4]. Variation in the charge heterogeneity has been shown to alter the *in vitro* and *in vivo* properties of mAbs [5]. To characterize their proteoforms, mAbs are either analyzed via bottom-up (peptide level), middle-up (reduction, fragments), or intact protein approaches [6]. Charge variant analysis (CVA) is typically conducted at the intact proteoform level. In addition, it requires limited sample preparation (typically only buffer exchange and/or dilution) avoiding the induction of additional modifications [7].

Several techniques have been described for CVA biopharmaceuticals [8], such as ion-exchange chromatography [9], capillary isoelectric focusing (cIEF) [10], and capillary zone electrophoresis (CZE) [11]. The latter is a well-established and accepted technique for mAb CVAs in the pharmaceutical industry. Selectivity in CZE is based on the differences in electrophoretic mobility, which is determined by charge and hydrodynamic radius or more precisely, protein charge-to-size ratio [12]. As the size of a mAb does not change significantly upon modification, CZE is very suitable to probe minor changes in the overall protein's charge. For efficient protein separation, the choice of an adequate capillary coating and background electrolyte (BGE) composition (type, pH, and ionic strength) is essential. By canceling out the electroosmotic flow (EOF) and adjusting the pH of the BGE to be close to the pI of the mAbs, the relative charge difference, and thus resolution, between proteoforms can be maximized [13]. However, when the pH is too close to the pI, migration will be too slow and solubility issues can occur [14–16].

In 2011, He *et al.* introduced a CVA method based CZE with UV absorbance detection which employed a dynamically coated fused-silica capillary using a BGE comprising of 400 mM ε-amino-caproic acid (EACA), 2 mM triethylenetetramine (TETA), and 0.05% m/v (hydroxypropyl) methylcellulose (HPMC) [17]. This method enables the separation of minor charge variants from the main isoform at a pH of 5.7. Its performance has been extensively validated and the approach has gained prominence for CVA in the pharmaceutical industry [18]. Although this CZE-UV method is efficient for quantification purposes in a quality control environment, it is not compatible with mass spectrometric detection and does not allow to characterize/identify separated peaks beyond the assignment of their acidic or basic nature. This limitation is rooted in the use of additives and non-volatile BGE constituents, which interfere with electrospray ionization (ESI), potentially causing ion suppression and contamination of the mass spectrometer [19].

Identification of proteoforms benefits greatly from the use of mass spectrometry (MS) [20]. The combination of CZE and MS is a valuable approach to facilitate the characterization of closely related and/or minor proteoforms that are difficult to distinguish by MS alone. Various CZE-MS methods for mAb analysis have been proposed, but the majority of these methods are performed under acidic conditions (acetic or formic acid at pH 2-3) as BGE yielding limited to no separation of charge variants [21].

In so-called native CZE-MS studies, a higher pH (*i.e.,* close to pH 7) is used [22]. So far, these

studies mostly focused on the separation of different proteins rather than CVA. CZE-MS methods applying a BGE of pH 5-7 are less common [23–25]. One notable exception is the use of commercial microfluidic (m) CZE-MS applications that use an MS-compatible BGE at a pH of 5.5, closely resembling the conditions of the EACA-based CZE-UV method of He *et al.* (2011) [26–29]. This mCZE-MS system provides high-throughput CVA, but unfortunately lacks optical detection, which limits its quantitative abilities. Hence, a flexible CZE-based method that enables mAb CVA combined with quantification via UV detection while also offering the capability of coupling with MS for charge variant identification has not been described yet.

In this study, we aimed to close this gap and developed a CZE-UV/MS system for intact mAb CVA. It makes use of a static neutral HPMC coating in order to prevent protein adsorption and suppress the EOF to maximize electrophoretic resolution [30]. To couple the CZE method with MS, we applied a recently introduced ESI nanoflow sheath liquid interface, referred to as "nanoCEasy" [31]. This interface results in higher detection sensitivity compared to traditional sheath liquid interfacing, enabling the detection of low abundant charge variants. In addition, the easy manipulation of the separation capillary and sheath liquid capillaries facilitates efficient capillary washing and BGE replacement during runs. In this study, the pH and concentration of the BGE buffer, CZE applied voltage, and quantity mAb were optimized for the CZE-UV method. Subsequently, the CZE-nanoCEasy-MS system was employed for the identification of resolved charge variants. The CZE-based method was evaluated by the analysis of various immunoglobin G (IgG) subclasses (IgG_1 and IgG_4) with isoelectric points (pI) between 7.4-9.2 and exhibiting diverse degrees of heterogeneity.

2. Experimental section

2.1 Chemicals

Methanol, isopropanol (MS-grade), water (MS-grade), and formic acid (MS-grade) were purchased from Biosolve (Valkenswaard, The Netherlands). Ammonium hydroxide solution (25%), and hydrochloric acid (37%) were acquired from Merck KGaA (Darmstadt, Germany). Sodium hydroxide, hydrofluoric acid (HF) (50.5%), calcium carbonate, HPMC, acrylamide, EACA, and TETA were purchased from Sigma-Aldrich (Zwijndrecht, The Netherlands). Acetic acid (glacial, p.a.) was purchased from Acros Organics (Geel, Belgium). Pembrolizumab, rituximab, and cetuximab were received from Amsterdam University Medical Center Pharmacy (Amsterdam, The Netherlands). Pembrolizumab (Keytruda®) was acquired from MSD (Kenilworth, New Jersey, USA). Rituximab (Trukima®) from Celltrion Healthcare (Amsterdam, The Netherlands). Cetuximab (Erbitux®) was acquired from Merck KGaA (Darmstadt, Germany). NISTmAb (reference material 8671, humanized IgG_{1k} monoclonal antibody) was purchased from the National Institute of Standards and Technology (Gaithersburg, Maryland, USA). Unless stated otherwise, the mAb samples were diluted to 1 $mg \cdot mL^{-1}$ in water.

2.2 Coating of separation capillary

For coating the capillary with HPMC, a procedure from Shen and Smith (2000) was adopted [32]. A bare fused silica capillary (50 µm i.d., 365 µm o.d., 60 cm as total length) was purchased from Polymicro Technologies (Phoenix, USA). The capillary was initially washed with methanol followed by flushing with water, 0.1 M sodium hydroxide, water, 0.1 M hydrochloric acid, and water at 100 $\mu L \cdot h^{-1}$ for five minutes each by using a syringe pump (kdScientific Legato 200, Massachusetts, USA). Between the steps, after flushing the capillary, the pH of the droplets coming out of the capillary was measured to control the basic and acidic conditions. Hereafter, 0.75% (w/v) HPMC solution was led through the capillary with a flow rate of 20 $\mu L \cdot h^{-1}$ for 40 minutes. Subsequently, the capillary was installed in a gas chromatography oven (Agilent Technologies, Waldbronn, Germany) in which the coating was heated under an inert nitrogen flow (3.5 bar) from 25 to 150 °C at 5 $°C \cdot min^{-1}$ for 45 minutes. After cooling

down to room temperature, each coated capillary was evaluated prior to analysis by measuring the EOF with 20 mM acrylamide, as an EOF marker. The BGE comprised 50 mM acetic acid (pH 2.8 and 5.0). Several pressures (10 – 100 mbar) were applied during the measurement to move the EOF in the direction of the detector. The CZE voltage was set to 30 kV. The coating was used when the EOF was below 10^{-9} $m^2 \cdot v^{-1} \cdot s^{-1}$ at pH 5.0.

2.3 Etching separation capillary

Safety precautions: HF is dangerous! Use appropriate safety procedures by using HF. Make use of a fume hood. Ensure that a calcium gluconate gel (2.5%) is nearby in case of exposure.

For CZE-MS, from 20 mm of the capillary outlet end, the polyimide layer was burnt off using a lighter. Subsequently, the bare fused silica capillaries end was etched with HF (50.5%) over a length of 10 mm as reported elsewhere [31]. The outlet opening was closed using a hot glue droplet to prevent the HF from accessing the capillary. The outlet end of the capillary was emersed in HF for approximately one hour to reduce the outer diameter of the capillary to < 150 µm. Note that polyimide should not come in contact with HF. To stop the reaction, the capillary was dipped in a saturated calcium carbonate solution to neutralize the HF and then washed with water. Before the CZE measurements, the blocked end with the glue droplet was cut off.

2.3 Instrumentation

2.3.1 CZE-UV

An Agilent 7100 CE system equipped with a diode array detector (DAD) (Agilent Technologies, Waldbronn, Germany) was used. The final BGE consisted of 50 mM acetic acid and adjusted to pH 5.0 using ammonium hydroxide. Other BGEs in this study were prepared in a similar fashion. Prior to each measurement, the capillary was conditioned by flushing with BGE for 200 s at 950 mbar. The samples were hydrodynamically injected for five seconds at 50 mbar (6.39 nL) followed by a BGE plug (five seconds, 50 mbar). High voltage (normal polarity mode) was ramped up to +25 kV in 0.2 minutes (generating a current of 30-35 µA). The maximum current was set to 60 µA as a safety measure. The capillary cassette temperature was set to 20 °C. The mAbs were detected at 214 nm with a data acquisition rate of 2.5 Hz. For storage of the capillary, the capillary was flushed with water and subsequently with air (300 s, 950 mbar) and stored at ambient temperature.

2.3.2. CZE-MS

The same Agilent 7100 CE system was used for CZE-MS measurements. The nanoCEasy interface was used to hyphenate the CE instrument to a Q Extactive Plus mass spectrometer (Thermo Fisher Scientific, Bremen, Germany) with an ESI source. In Supplementary Information, Fig. S1 and S2 show the configuration of the nanoCEasy interface. Briefly, the nanoCEasy interface employs two modes: (i) conditioning mode in which the separation capillary is moved backward during flushing of the BGE, and (ii) separation mode in which the separation capillary is moved forward to around 1.4 mm from the emitter tip [31]. Glass emitters with a length of 55 mm with a length point of 3 mm and an emitter i.d. of about ~ 30 µm were used (Biomedical Instruments Pipettes, Zöllnitz, Germany). The distance between the emitter tip and the MS orifice was set to 3 mm. The second capillary (100 µm i.d., 245 µm o.d., 30 cm length) was filled with sheath liquid composed of 0.5% formic acid in 50/50 isopropanol/water. A syringe pump was used with a flow rate of 10 $\mu L \cdot min^{-1}$. The nanoCEasy setup was controlled using a digital microscope (Dino-Lite, Almere, The Netherlands). For the MS, the electrospray voltage was 2100 V (positive ion mode), microscans were set to 10 ms, in-source CID was 80 eV, sweep gas flow rate was 3 Arb, capillary temperature was 275 °C, S-lens RF level was 100, and

scan range was set to 1500-6000 *m/z* with a resolution of 17,000. The CE voltage was ramped up to +20 kV in 0.2 minutes (generating a current of 30-35 μA).

2.3.3 EACA-based CZE-UV method

The CZE method using a BGE containing, amongst others, EACA was used as reported by He *et al*. [17] with the calculated settings for Agilent 7100 CE system of Wiesner *et al.* [18]. In short, a bare fused-silica capillary (50 μm i.d., 365 μm o.d., 60 cm as total length) was used. The procedure of making BGE was described by Wiesner *et al.* [18]. The separation voltage was ramped up from 0 to +30 kV in 0.20 minutes. The capillary cassette temperature was set to 25 °C. The samples were injected by applying 35 mbar for five seconds. The UV detector was set to 214 nm with 10 Hz as the data acquisition rate.

2.4 Data processing

CE data were processed and integrated using OpenLAB CDS software (Agilent Technologies, Waldbronn, Germany). For visualization purposes, baseline correction was executed utilizing the arPLS algorithm [33]. Previous studies have demonstrated the efficacy of this algorithm across diverse experimental conditions [34]. The raw MS data were visualized in Thermo Fisher Scientific Freestyle software (Thermo Fisher Scientific, Bremen, Germany). For the deconvolution of the spectra and calculation of the average mass, Unidec (University of Arizona, Phoenix, USA) was used [35]. CZE-MS data are available at MassIVE: ftp://massive.ucsd.edu/v07/MSV000094521/.

3. Results and Discussion

Four different mAbs were selected to evaluate whether the proposed method can assess various common modifications. The selected antibodies were rituximab, cetuximab, NISTmAb, and pembrolizumab. Together, they span a broad pI range (7.4-9.4), various subclasses (IgG_1 and IgG_4), and a large diversity of PTMs (*e.g.*, sialylation, deamidation, C-terminal lysine clipping). Table S1 summarizes their properties in more detail.

3.1 Basic performance of HPMC coating

Efficient intact protein analysis requires the use of coated capillaries in order to minimize the protein interaction with the capillary wall which may lead to band broadening and even complete protein adsorption [36]. In this study, an HPMC-coated capillary was used for this purpose. This coating also suppresses the EOF (μ_{EOF}~0), thereby potentially allowing efficient electrophoretic separation of the charge variants based on their difference in mobility [36].

The suppression of EOF by the HPMC-coated capillaries was evaluated using acrylamide (EOF marker) under different applied pressures ranging from 10 to 100 mbar using 50 mM acetic acid pH 2.8 and 5.0. During the measurements, a voltage of 30 kV was applied. Subsequently, the EOF velocity was calculated by plotting the reciprocal measured migration times against the applied pressure and extrapolating to zero pressure (Fig. S3). The EOF mobility was subsequently calculated from three replicates per pressure. Both at 50 mM acetic acid pH 2.8 and pH 5.0, they were nearly zero ($7.5 \cdot 10^{-10}$ $m^2 \cdot v^{-1} \cdot s^{-1}$ (RSD= 6.4%, n=3) and $7.1 \cdot 10^{-10}$ $m^2 \cdot v^{-1} \cdot s^{-1}$ (RSD= 3.7%, n=3)), which is more than one order lower than the EOF mobility of bare fused silica capillaries ((50 mM acetic acid pH 5.0, $1.9 \cdot 10^{-8}$ $m^2 \cdot v^{-1} \cdot s^{-1}$ (RSD= 2.4%, n=3).[37]

3.2 Optimization of CZE method: BGE pH and concentration, and separation voltage

The separation performance of the charge variants was optimized by varying the following parameters: (i) pH of BGE (2.8, 4.0, 5.0, 5.8) and (ii) concentration of BGE (10 – 100 mM acetic acid). Acetic acid was used as a BGE constituent due to its proven compatibility with mass spectrometric detection. First,

the effect of the pH of the BGE on the separation of four mAbs was evaluated. The BGE concentration was 50 mM acetic acid in all cases while applying 25 kV as separation voltage. The results obtained for pembrolizumab are depicted in Fig. 1. Electropherograms for the other three mAbs are reported in Fig. S5, and a summary of the results is reported in Table S2. All the measurements are done in triplicate.

As shown in Fig. 1A and S5, the pH of the BGE strongly affects the separation of the charge variants. At pH 2.8, there are no charge variants resolved from the main isoform for pembrolizumab. Whereas at pH 5.0 and 5.8, five or six charge variants are resolved from the main isoform. The mAb and its variants migrate slower as the pH approaches the pI of the mAb due to their reduced net charge and thus decreased electrophoretic mobility. Therefore potential electrophoretic mobility differences between charge variants depend on their net charge as these variants have the same size. The electrophoretic mobility difference is relatively small at low pH (e.g. pH 3), especially for acidic variants as these are (partially) protonated at low pH. In contrast, increasing the pH to a value close to the mAb pI reduces the net charge of the antibody and increases the electrophoretic mobility differences between charge variants, resolving basic variants, main isoform, and acidic variants. The basic variants are migrating at first due to the introduction of extra positive charges to the antibody [5,38]. The main isoform and acidic variants migrate slower due to their decrease in lower pI. For example, deamidation introduces negative charges to the antibody and gives it a net lower positive charge [39]. For the best separation, the difference in electrophoretic mobilities of the charge variants should be maximized to improve the resolution. The best separation with the most resolved charge variants for the mAbs was achieved at pH 5.0 and 5.8. However, for further optimization, Acetic acid at pH 5.0 was chosen as optimal due to the lower CZE current (30-35 µA vs >60 µA) which was preferable for the CZE-MS measurements.

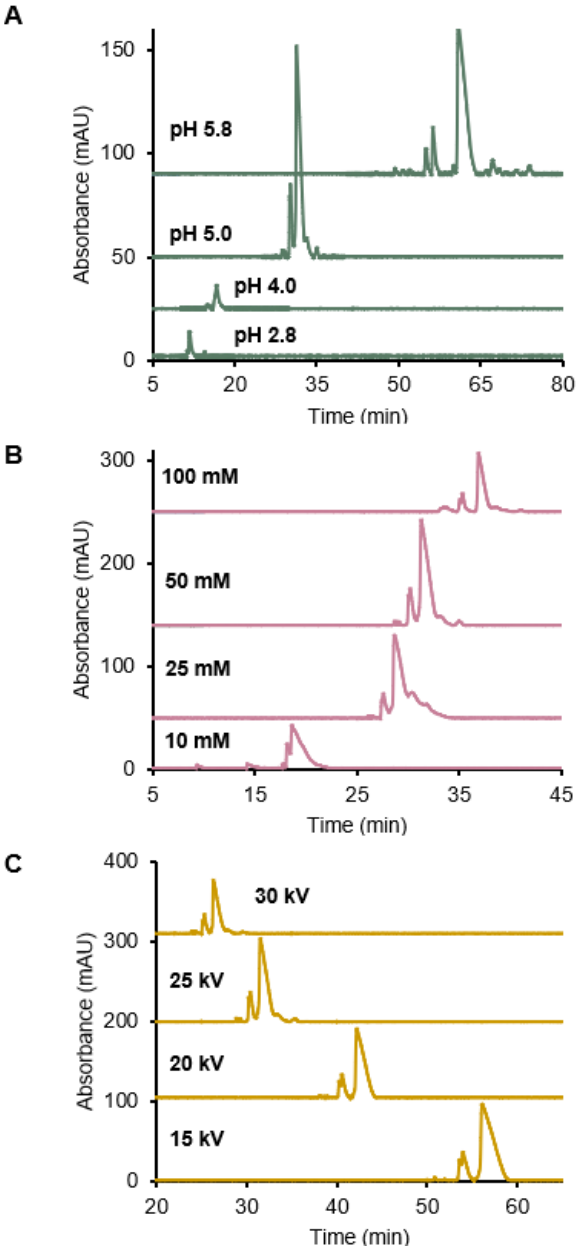

Fig. 1: CZE-UV analysis of pembrolizumab (1.0 mg·mL^{-1}) using (A) BGEs of 50 mM acetic acid set to various pH values (2.8-5.7), (B) BGE at various acetic acid conditions (10-100 mM) set to pH 5.0, and (C) a BGE of 50 mM acetic acid set to pH 5.0 applying various voltages (15-30 kV). Conditions: HPMC-coated capillary (50 μm i.d. x 60 cm), BGE 50 mM acetic acid pH 5.0 (unless stated otherwise), separation voltage 25 kV (A and B). See paragraph 2.3.1 for additional CE conditions.

As a next step, different BGE concentrations (10 – 100 mM acetic acid adjusted to pH 5.0) were tested (Fig. 1B and S5). Fig. 1B shows a noticeable shift in migration time across these various BGE concentrations. The lowest BGE concentration (10 mM) led to a diminished electrophoretic resolution among the charge variants. Conversely, higher ionic strength resulted in lower effective mobility, thereby maximizing the difference in electrophoretic mobility and therefore allowing for better separation efficiency. The number of resolved charge variants has a significant increase at a higher BGE concentration (50-100 mM). For example, using 10 mM acetic acid pH 5.0, no acidic variants were resolved from the main isoform, whereas with 100 mM acetic acid pH 5.0, three acidic variants were separated from the main isoform (Fig. 1B). Cetuximab has several different sialylated proteoforms which has a negative charge and can be separated with this method. At 100 mM acetic acid pH 5.0, six acidic variants could be separated whereas at a lower BGE concentration (10 mM) only two acidic

variants were separated (Fig. S6). This trend of more resolved charge variants at higher BGE concentrations was also noticeable for the other mAbs. Nevertheless, peak broadening may occur as a result of reduced ion mobility. The best separation was achieved at 50 and 100 mM acetic acid pH 5.0 (highest plate numbers (Fig. 2). However, high BGE concentration can lead to high CE current. With 100 mM acetic acid adjusted to pH 5.0, the CE current was above 60 µA which is not preferred due to the risk of joule heating. Therefore, 50 mM acetic acid pH 5.0 was chosen as the optimal BGE concentration.

Furthermore, to speed up the analysis of the charge variant, various applied voltages (15-30 kV) were tested under the optimal conditions (50 mM acetic acid pH 5.0). In general, the higher the electric field, the faster the ion migration (Fig. 1C) and the higher the current of the method (e.g. 30 and 15 µA were observed for 30 and 15 kV applied during separation). Short separation times inherently enhance separation efficiency as diminished diffusion correlates with reduced peak broadening. Additionally, higher CE voltages facilitated higher plate numbers for certain mAbs (rituximab and pembrolizumab) when a higher voltage is applied due to the smaller peak widths (Fig. 2 and S7). For instance, at 15 kV, the full width at half maximum (FWHM) of the main isoform peak from cetuximab is 20% broader compared to the FWHM of cetuximab measured at 30 kV. A lower voltage may result in more peak overlapping which is not desirable (Table S2). Notably, at higher applied voltages, the same number of resolved basic and acidic variants was observed (Fig. S6).

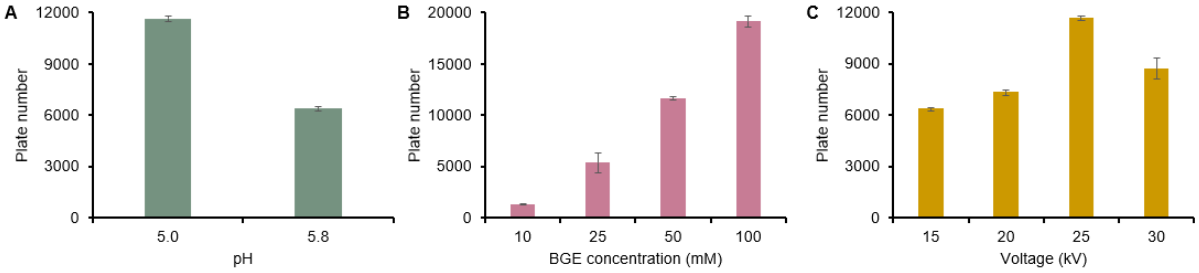

Fig. 2: Plate numbers calculated from the FWHM of pembrolizumab (1.0 mg·mL^{-1}) under various conditions (A) BGEs of 50 mM acetic acid set to various pH values (5.0-5.7), (B) BGE at various acetic acid conditions (10-100 mM) set to pH 5.0, and (C) a BGE of 50 mM acetic acid set to pH 5.0 applying various voltages (15-30 kV). Conditions: HPMC-coated capillary (50 µm i.d. x 60 cm), BGE 50 mM acetic acid pH 5.0 (unless stated otherwise), separation voltage 25 kV (A and B). See paragraph 2.3.1 for additional CE conditions.

Finally, the repeatability of the developed method (50 mM acetic acid pH 5.0) was assessed. The stability of the coating was tested with a BGE of 50 mM acetic acid adjusted to pH 5.0 using ammonium hydroxide. Pembrolizumab was measured five times with both buffer pHs over two consecutive days (Fig. S2). The RSD of the migration time of the main isoform for intraday repeatability (n=5 measurements) was 0.3%. For interday repeatability (n=5 measurements), an RSD was 2.1% at pH 5.0. The repeatability of the HPMC coating procedure was also tested by measuring pembrolizumab (n=5 measurements) with three HPMC capillaries at pH 5. The RSDs of the migration time (n=3 HPMC coated capillaries) were 1.7%, indicating low variance between HPMC capillaries. The lifespan of the HPMC capillary coating has not been statistically determined. However, based on the number of measurements that have been run on one HPMC capillary for the optimization of the CZE method. The lifespan was at least 40 runs.

In the previous experiments, we optimized the CZE method using a mAb concentration of 1 mg·mL^{-1}, which corresponds with 6.4 ng analyte when 6.4 nL was injected. A higher sample load may be useful for detecting less abundant proteoforms. Therefore, we investigated the CZE separation performance for mAbs as a function of injected concentrations (0.1 to 5 mg·mL^{-1}), as shown in Fig. 3 and S8. The samples were diluted in water.

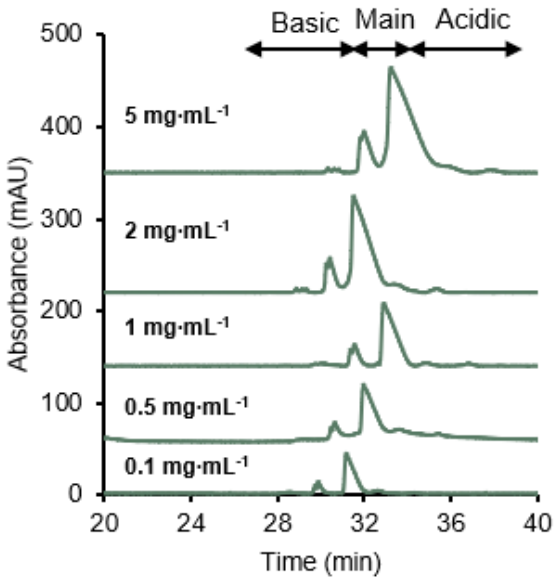

Fig. 3: CZE-UV analysis of pembrolizumab measured at different injected concentrations (0.1 mg·mL^{-1}, 0.5 mg·mL^{-1}, 1 mg·mL^{1}, 2 mg·mL^{-1}, and 5 mg·mL^{-1}). Conditions: HPMC-coated capillary (50 µm i.d. x 60 cm), BGE 50 mM acetic acid pH 5.0, separation voltage 25 kV. See paragraph 2.3.1 for additional CE conditions.

In pharmaceutical analysis, maintaining separation performance is of paramount importance, even when dealing with elevated quantities of injected mAb. Fig. 3 shows that at higher injected concentrations of mAb, the charge variant resolution decreases. Fig. S9 provides an overview of the number of peaks that are detected at various injected concentrations of different mAbs. The acidic variants, in particular, overlap more with the main isoform at a higher injected concentration (5 mg·mL^{-1}), but the concentration of mAb does not have a significant impact on the separation of basic variant peaks. The FWHM was observed to be larger at higher injected concentrations. Additionally, the plate number was significantly increased at a lower injected concentration compared to a higher injected concentration. For instance, the plate number required for 0.1 mg·mL^{-1} of pembrolizumab was 4.8 times greater than for 5 mg·mL^{-1} (Table S3). In conclusion, the separation performance can be maintained when an injected concentration of 0.1-2 mg·mL^{-1} is used. However, at a higher injected concentration (*e.g.,* 5 mg·mL^{-1}), the acidic variants may overlap with the main isoform, whereas the basic variants remain separated from the main isoform.

3.3 Comparison with established EACA-based CZE-UV method

The EACA method of He *et al.* is commonly used in the pharmaceutical industry [17]. To benchmark our developed method the four mAbs described in this study were applying the method described by He *et al.* [17]. Fig. 4A compares the overall profile of the relative abundances of the charge variants of the four analyzed mAbs as determined with the EACA method and our MS-compatible method. There is a clear correlation between the values obtained with both methods (R^2 of 0.9759), indicating that the methods' capacity to distinguish charge variants from the main isoform is similar. Both methods used an injected sample concentration of 1 mg·mL^{-1}. For 1 mg·mL^{-1} NISTmAb, the relative abundance of the basic variants was lower than that obtained with the EACA method. However, when lowering the injected concentration to 0.5 mg·mL^{-1}, the two methods produced similar relative abundances for the charge variants. This may be attributed to capillary overloading which may decrease the resolution between charge variants and main isoform, as also shown in the previous section. Still, the relative abundance obtained with the two methods was similar. The largest difference in relative abundance was observed for rituximab (Table S4), which exhibited a relative abundance of the main isoform of 79.3% and 70.3% using the EACA and the method here described, respectively. This deviation comes

from that the EACA method provides a better separation of the basic and acidic variants from the main isoform compared to the MS-compatible method (Fig. S10). For example, Fig. 4B shows that the basic variants have higher resolution with the EACA method compared to our MS-compatible method. However, the relative abundances of the basic variants of pembrolizumab (14.5% (EACA method) and 15.8% (our method)) seem to be similar in both methods. For the other antibodies, the difference in the relative abundance of the charge variants determined with both methods was never more than 5.9%. While the percentages of charge variants align closely with the literature, they may diverge depending on the analytical techniques and methodologies, as mentioned by Goyon *et al.* (2017) [40]. Our MS-compatible method may introduce overlaps between basic and acidic variants with the main isoform, altering relative percentages of the charge variants. Withal, the relative abundances of the charge variants measured under the conditions of both methods seem to be similar.

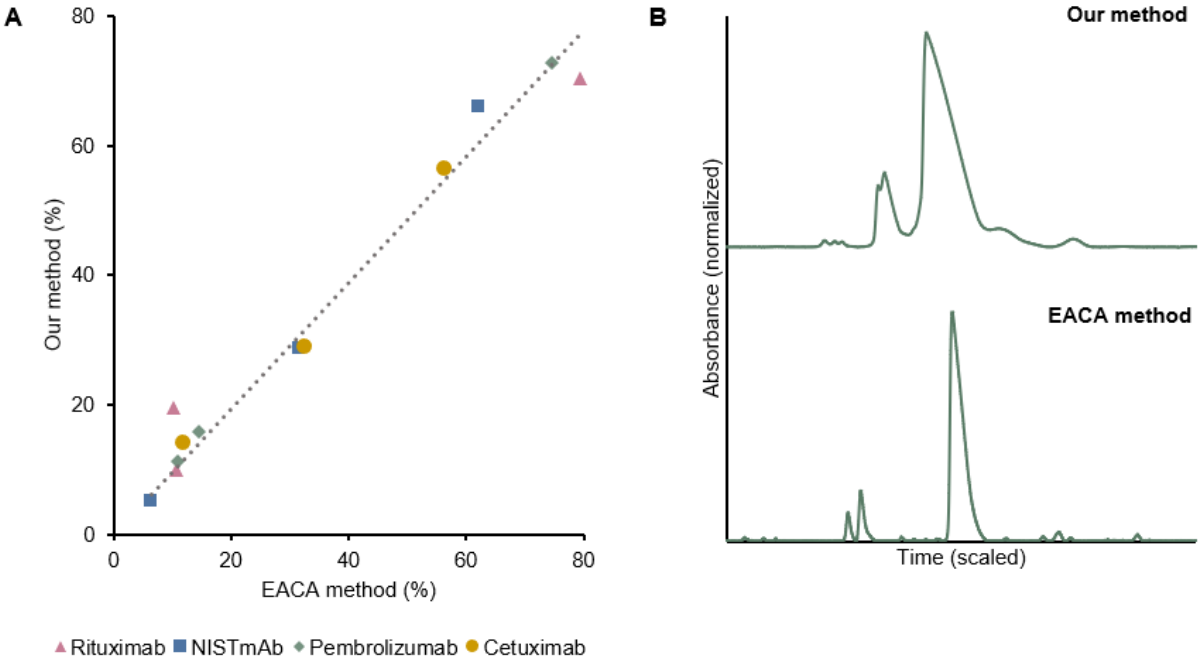

Fig. 4: (A) Relative abundance of the charge variants of rituximab (pink, triangle), NISTmAb (blue, square), pembrolizumab (green, diamond), and cetuximab (yellow, circle) measured with our MS-compatible method (y-axis) and EACA method from He *et al.* (2011) (x-axis). A trendline (intercept=0) is plotted (grey, dots) to show the differences in relative abundances of the charge variants (%) between both methods. (B) CZE-UV analysis of 1 mg·mL^{-1} pembrolizumab was measured under the conditions of our method (top, section 2.3.1 for detailed information) and the EACA method (bottom, see section 2.3.3. for detailed information). The absorbance of the y-axis is normalized and the time on the x-axis is scaled.

3.4 Profiling of mAbs by CZE-MS

The nanoCEasy interface was implemented to couple the CE instrument to the MS instrument [31]. In our final method, the sheath liquid consisted of 0.5% formic acid in 50% isopropanol, which provides MS denaturing conditions for the mAb. Initially, acetonitrile and methanol were also tested as organic solvents in the sheath liquid (Fig. S11), however, with isopropanol, a higher signal intensity was obtained for the mAbs. For acetonitrile, more adducts were present. The composition of the sheath liquid was not extensively studied in this study (*e.g.,* ratio aqueous/organic solvent, percentage acid, etc.). The syringe pump for the sheath liquid was set to 10 μL/min, however, only > 100 nL/min sheath liquid will enter the emitter tip [31]. The rest of the flow will flush backward to waste as shown in Fig. S1.

In this study, the Q Exactive Plus MS instrument was employed. This instrument lacks grounding in its ionization source. Consequently, the current originating from the CE instrument

correlates directly with the MS spray current and needs to be taken into account for safety precautions. For instance, if the measured CE current is 30 µA, the MS spray current will be of a similar magnitude. It is worth noting that the CE current is measured at a single point rather than across the entire system, potentially allowing for higher CE currents than those monitored at any given moment. Considering the coupling with MS, the use of a BGE buffer containing 50 mM acetic acid pH 5.8 or 100 mM acetic acid pH 5.0 could lead to an elevated CE current (> 60 µA). Therefore, for the separation of the charge variants with CZE-MS, 50 mM acetic acid at pH 5.0 was chosen as an optimal BGE composition. An additional challenge was encountered when the MS spray current was high (*e.g.*, 30 µA), resulting in the actual MS voltage (>2.1 kV) dominating the applied MS voltage (2.1 kV), resulting in an unstable ionization. This seems to come from the high current. To address this problem, the CE voltage was reduced to 20 kV in order to gain control of the actual MS voltage and to ensure a stable ionization spray.

The pH of the BGE is adjusted using ammonium hydroxide, which causes the CE current. A high concentration of ammonium (> 5 mM) in the BGE can pose a challenge for CZE coupling to MS. Besides the negative effect on the current, ammonium hydroxide also suppresses the protein ionization and reduces the sensitivity of the method [41]. With traditional sheath liquid interfaces (µL/min sheath liquid flow), the dilution factor is higher compared to the nanoflow sheath liquid interface (nL/min sheath liquid flow) used in this study. Despite the gain in sensitivity thanks to the nanoCEsy interface, the dilution and the ionization suppression of ammonium hydroxide resulted in relatively high concentrations of mAbs required to get satisfactory MS measurements [24]. For the mAb tested 1 $mg \cdot mL^{-1}$ was chosen except for Cetuximab for which a higher concentration (2 $mg \cdot mL^{-1}$) was needed due to its higher heterogeneity.

The detection of low abundant proteoforms, *e.g.*, due to oxidation and deamidation in mAbs is crucial despite their relative abundance of less than one percent of 150 kDa. As shown in previous figures, we are able to separate the basic variants from the main isoform. By using CZE-MS, the charge variants could be identified. Fig. 5 shows the extracted ion electropherograms (EIEs) of the major charge variants of NISTmAb and pembrolizumab. The m/z values that were used to generate the EIEs of the four mAbs are listed in Table S5. Fig. S12 and S13 show the EIEs of rituximab and cetuximab, respectively. The theoretical and measured masses of the charge variants are listed in Table S6. The detection limit, based on the peak area of pembrolizumab, is about 6 µg/mL. This allows proteoforms with an intensity of < 1% to be detected.

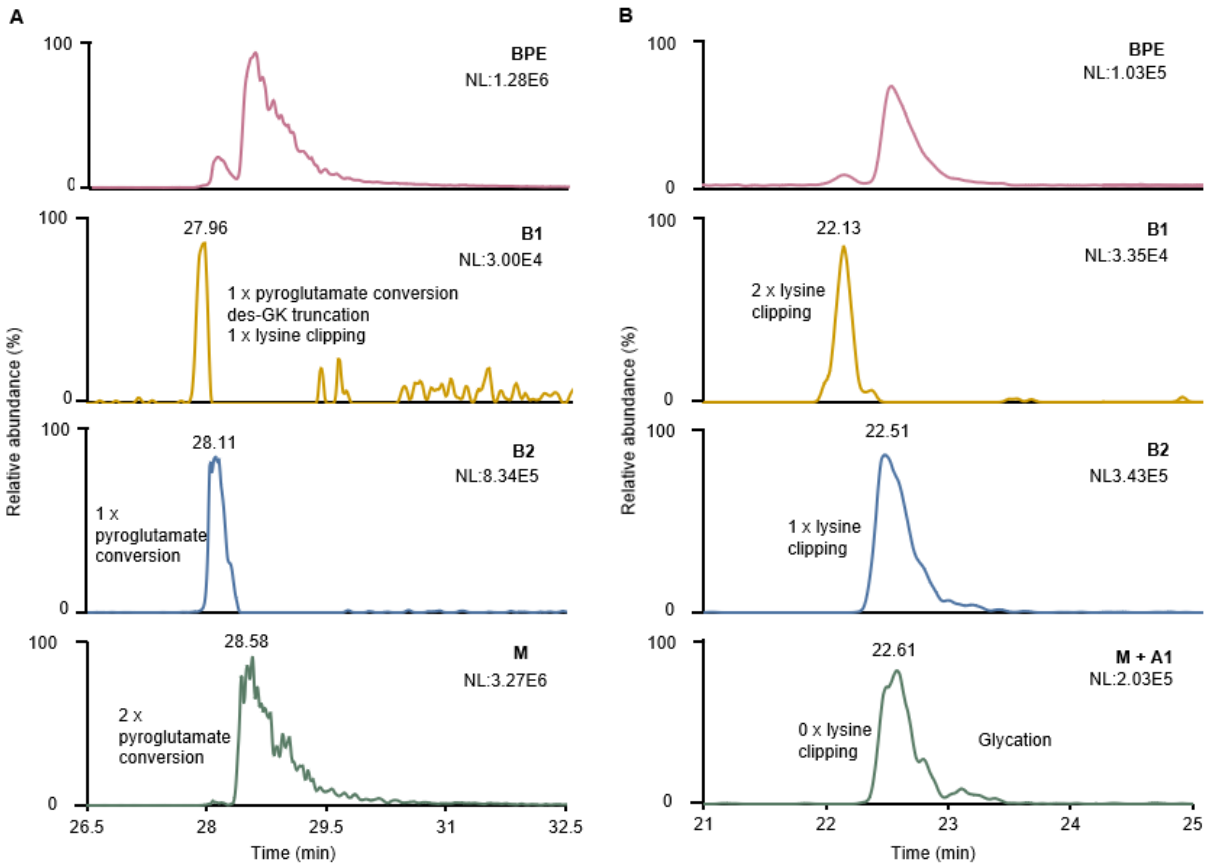

Fig. 5: Separation of charge variants of (A) pembrolizumab and (B) NISTmAb with CZE-MS. The base peak electropherogram (BPE) and EIEs of the basic (B1 and B2), main (M), and acidic (A1) variants are plotted. The charge modifications are assigned in this figure. The m/z values of the EIEs are listed in Table S5. Conditions: HPMC-coated capillary (50 µm i.d. x 60 cm), BGE 50 mM Acetic acid pH 5.0, separation voltage 20 kV. See paragraphs 2.3.1 and 2.3.2 for detailed CE and MS settings.

For rituximab, NISTmAb, and pembrolizumab, the basic variants could be extracted from the main isoform. For NISTmAb, two basic variants were assigned to C-terminal lysine variants (K) based on the obtained mass spectra. The second basic variant peak (B2) overlaps with the main peak (M) but could be extracted based on the MS data (Fig. 5). The basic variant peaks showed a positive mass offset of one or two times 128 Da (peak B1 (148,461.5 Da, 2 K) and B2 (148,330.0 Da, 1 K) compared to the main isoform peak. This suggested that incomplete C-terminal lysine clipping had occurred. For assigning the glycoforms, the nomenclature of the glycoforms was used as reported by Lippold *et al. (2019)* [42]. Between glycoform G1F/G1F or G0F/G2F of the main isoform (148,364.0 Da, M) and acidic variant peak (148,524.8 Da, A), there was a mass difference of +160 Da which is in accordance with the addition of hexose sugar (162 Da). This glycation takes place on a lysine resides [43]. Furthermore, the mass difference of the acidic variant (G1F/G1F or G0F/G2F + glycation) between the calculated mass (148,523.5 Da) and the measured mass (148,524.8 Da) is 1.3 Da. This could be a deamidation variant. However, due to the small mass difference of deamidation (1 Da), it is very challenging to identify it [44]. The detection of lysine, glycation, and deamidation of NISTmAb is consistent with the literature [45]. The experimental masses with the identified PTMs are represented in Table S6. Some masses exhibit larger mass errors (> 5 Da). This is especially true for the basic variant (B1) due to the lower intensity and more noise.

To our knowledge, it is the first time that pembrolizumab has been analyzed with CZE-MS. Two basic variants could be extracted from the main peak. Des-GK truncation was found in the basic variant peak (B1) resulting in a -185 Da mass shift compared to the main isoform. des-GK truncation is a PTM that can be detected in the IgG_4 subclass [46]. It can also be observed in the other IgG subclasses, but

it is to a much lesser extent in contrast to the IgG_4 subclasses. C-terminal lysine clipping was also observed in the basic variants. The second basic variant peak of pembrolizumab (148,907.0 Da, B2) has a mass difference of 17 Da which indicates cyclization to pyroglutamate. The main peak (148890.3 Da, M) contains one cyclization of N-terminal glutamine to pyroglutamate (Gln → pyro-Glu) on each heavy chain. These modifications are in agreement with a recent study by Zhang *et al.* (2023) in which pembrolizumab was measured using imaged cIEF [47]. For most of the antibodies, the glutamine conversion to pyroglutamate is quite common when the beginning of the heavy chain contains the amino acid glutamine (Q). To determine deamidation variants, the antibodies were also measured at 35,000 resolution. However, only for pembrolizumab multiple deamidation variants could be determined due to a mass difference of 1 Da, *e.g.*, main isoform (149,376.9 Da (G1F/G2F)) and acidic variant (149,378.1 Da (G1F/G2F with possible deamidation). This small mass difference was also the case for two other glycoforms. For the rest of the identified glycoforms, the mass difference was around 2-3 Da (Table S7). Studying the antibodies at the middle-up or bottom-up level can help in understanding the deamidation [44].

A majority of the antibodies contain zero or two conversions to pyroglutamate. However, rituximab contains four times pyroglutamate (two times on the heavy chain, and two times on the light chain) [48]. There is no variation in pyroglutamate over the basic variant peaks. Nonetheless, rituximab has two C-terminal lysine variants on the heavy chain which are separated in the basic variant region (B1 and B2) (Fig. S12). Besides lysine variants, oxidation was also identified in the basic variant peaks (Table S6). Furthermore, glycoforms containing sialic acids (N-Acetylneuraminic) were identified. However, there was a significant large mass error (38 Da or 70 Da) for these more acidic glycoforms (G1F/G2FS1, G1F/G2FS2, G2F/G2FS1, G2F/G2FS2). In 2021, Di Macro *et al.* measured rituximab as well and also faced large mass errors for the sialic acids [49]. Also for rituximab, there is no explanation for why these mass errors are significantly larger compared to the other glycoforms. For some PTMs in the basic variants (*e.g.*, B2), there is also a large mass error (>5 Da). This may be due to the low signal-to-noise for these less abundant variants.

Lastly, cetuximab is more heterogeneous due to the four glycosylation sites in the Fc and Fab domains. Next to that, cetuximab also contains sialic acids which add an extra negative charge to the antibody [50]. Therefore, it is challenging to separate the charge variants from each other. Each peak can have isomers which makes the data more complex. With our method, we are able to resolve the basic and acidic variant peaks from the main peak. The basic variant peaks showed a mass difference of one or two times ~128 Da (Fig. S13 and Table S6). The acidic variants contain fucose and/or sialic acid monosaccharides.

4. Conclusion

From the CQA perspective, it is crucial to monitor charge variants of mAbs. With the CZE-based EACA method of He *et al.* (2011), charge variants can be separated and quantified by optical detection. Nonetheless, the identification of these variants by MS is not possible due to the non-volatile BGE. Our developed method not only facilitates relative quantification via optical detection but also enables hyphenation with MS to identify charge variants. This can be beneficial from the CQA perspective. Using a higher pH (*e.g.*, pH 5.0 or 5.8), the charge variants were more effectively separated from the main isoform compared to the typical acidic pH (*e.g.*, pH 2.8) conditions used for CZE-MS of proteins. However, the high concentrations of ammonium needed to adjust the pH can suppress the ionization. Therefore here we report the use of the nanoCEasy interface, which thanks to its low flow regime, allowed us to measure and identify the charge variants. The method was tested with antibodies in the pI range of 7.4-9.4, variation in IgG subclasses (IgG_1 and IgG_4), and with varying degrees of heterogeneity. Thanks to the selectivity of this method, the separation of low-abundant species, such as C-terminal lysine (less than 10% relative abundance to the main isoform) could be achieved, all at

an intact level. No sample preparation was necessary. A correlation exists in terms of the relative abundances of the charge variants acquired through the CZE-UV EACA method of He *et al.* and our method. However, the acidic variants overlapped more with the main isoform with our CZE-UV method than with the EACA method. It is important to note that with the EACA method, MS detection is not possible due to the use of non-volatile buffers. Our CZE-UV/MS method shows flexibility as it can be used for relative quantification as well as identification of the charge variants due to the use of volatile BGE buffers. This highlights the potential of this CZE-UV/MS method to be a valuable tool for in-depth mAb charge variant characterization.

CRediT author statement

Annika A.M. van der Zon: Conceptualization, Methodology, Investigation, Visualization, Writing-original draft, **Alisa Höchsmann:** Resources, Collaboration, **Tijmen S. Bos:** Data curation, **Christian Neusüß:** Resources, Collaboration, **Govert W. Somsen:** Writing-Review & Editing, **Kevin Jooß:** Experimental planning, Supervision, Writing-Review & Editing, **Rob Haselberg:** Conceptualization, Writing-Review & Editing, **Andrea F.G. Gargano:** Experimental planning, Supervision, Writing-Review & Editing, Funding acquisition

Acknowledgments

This work was performed within the Centre for Analytical Sciences Amsterdam (CASA). The fruitful discussions are gratefully acknowledged. The authors would like to thank Jesper Ruiter (Vrije Universiteit Amsterdam, CASA) for the preliminary experiments on the HPMC coating and Johannes Schlecht (Agilent Technologies) for his help with the nanoCEasy interface.

Appendix A. Supplementary data

Supplementary data related to this article can be found, in the online version.

Conflict of interest

The authors declare no conflict of interest.

6. References

[1] Sharma P, Joshi R V., Pritchard R, Xu K, Eicher MA. Therapeutic Antibodies in Medicine. Molecules 2023;28:6438. https://doi.org/10.3390/molecules28186438.

[2] Liu H, Gaza-Bulseco G, Faldu D, Chumsae C, Sun J. Heterogeneity of Monoclonal Antibodies. J Pharm Sci 2008;97:2426–47. https://doi.org/10.1002/jps.21180.

[3] Gupta T, Kumar A, Seshadri S. Bioprocess Challenges in Purification of Therapeutic Protein Charge Variants. Biotechnology and Bioprocess Engineering 2023;28:493–506. https://doi.org/10.1007/s12257-023-0078-4.

[4] Beck A, Liu H. Macro- and Micro-Heterogeneity of Natural and Recombinant IgG Antibodies. Antibodies 2019;8:18. https://doi.org/10.3390/antib8010018.

[5] Du Y, Walsh A, Ehrick R, Xu W, May K, Liu H. Chromatographic analysis of the acidic and basic species of recombinant monoclonal antibodies. MAbs 2012;4:578–85. https://doi.org/10.4161/mabs.21328.

[6] van der Zon AAM, Verduin J, van den Hurk RS, Gargano AFG, Pirok BWJ. Sample transformation in online separations: how chemical conversion advances analytical technology. Chemical Communications 2024;60:36–50. https://doi.org/10.1039/D3CC03599A.

[7] Pot S, Gstöttner C, Heinrich K, Hoelterhoff S, Grunert I, Leiss M, et al. Fast analysis of antibody-derived therapeutics by automated multidimensional liquid chromatography – Mass spectrometry. Anal Chim Acta 2021;1184:339015. https://doi.org/10.1016/j.aca.2021.339015.

[8] Kaur H, Beckman J, Zhang Y, Li ZJ, Szigeti M, Guttman A. Capillary electrophoresis and the biopharmaceutical industry: Therapeutic protein analysis and characterization. TrAC Trends in Analytical Chemistry 2021;144:116407. https://doi.org/10.1016/j.trac.2021.116407.

[9] Fekete S, Beck A, Veuthey J-L, Guillarme D. Ion-exchange chromatography for the characterization of biopharmaceuticals. J Pharm Biomed Anal 2015;113:43–55. https://doi.org/10.1016/j.jpba.2015.02.037.

[10] Xu T, Sun L. A Mini Review on Capillary Isoelectric Focusing-Mass Spectrometry for Top-Down Proteomics. Front Chem 2021;9. https://doi.org/10.3389/fchem.2021.651757.

[11] Dadouch M, Ladner Y, Perrin C. Analysis of Monoclonal Antibodies by Capillary Electrophoresis: Sample Preparation, Separation, and Detection. Separations 2021;8:4. https://doi.org/10.3390/separations8010004.

[12] Jooß K, McGee JP, Melani RD, Kelleher NL. Standard procedures for native CZE-MS of proteins and protein complexes up to 800 kDa. Electrophoresis 2021;42:1050–9. https://doi.org/10.1002/elps.202000317.

[13] Haselberg R, De Vijlder T, Heukers R, Smit MJ, Romijn EP, Somsen GW, et al. Heterogeneity assessment of antibody-derived therapeutics at the intact and middle-up level by low-flow sheathless capillary electrophoresis-mass spectrometry. Anal Chim Acta 2018;1044:181–90. https://doi.org/10.1016/j.aca.2018.08.024.

[14] Kiraga J, Mackiewicz P, Mackiewicz D, Kowalczuk M, Biecek P, Polak N, et al. The relationships between the isoelectric point and: length of proteins, taxonomy and ecology of organisms. BMC Genomics 2007;8:163. https://doi.org/10.1186/1471-2164-8-163.

[15] Menon MK, Zydney AL. Measurement of Protein Charge and Ion Binding Using Capillary Electrophoresis. Anal Chem 1998;70:1581–4. https://doi.org/10.1021/ac970902r.

[16] Meyer S, Clases D, Gonzalez de Vega R, Padula MP, Doble PA. Separation of intact proteins by capillary electrophoresis. Analyst 2022;147:2988–96. https://doi.org/10.1039/D2AN00474G.

[17] He Y, Isele C, Hou W, Ruesch M. Rapid analysis of charge variants of monoclonal antibodies with capillary zone electrophoresis in dynamically coated fused-silica capillary. J Sep Sci 2011;34:548–55. https://doi.org/10.1002/jssc.201000719.

[18] Wiesner R, Zagst H, Lan W, Bigelow S, Holper P, Hübner G, et al. An interlaboratory capillary zone electrophoresis-UV study of various monoclonal antibodies, instruments, and ε-aminocaproic acid lots. Electrophoresis 2023;44:1247–57. https://doi.org/10.1002/elps.202200284.

[19] Alhazmi HA, Albratty M. Analytical Techniques for the Characterization and Quantification of Monoclonal Antibodies. Pharmaceuticals 2023;16:291. https://doi.org/10.3390/ph16020291.

[20] Schaffer L V., Millikin RJ, Miller RM, Anderson LC, Fellers RT, Ge Y, et al. Identification and Quantification of Proteoforms by Mass Spectrometry. Proteomics 2019;19. https://doi.org/10.1002/pmic.201800361.

[21] Nagy C, Andrási M, Hamidli N, Gyémánt G, Gáspár A. Top-down proteomic analysis of monoclonal antibodies by capillary zone electrophoresis-mass spectrometry. Journal of Chromatography Open 2022;2:100024. https://doi.org/10.1016/j.jcoa.2021.100024.

[22] Schwenzer A, Kruse L, Jooß K, Neusüß C. Capillary electrophoresis-mass spectrometry for protein analyses under native conditions: Current progress and perspectives. Proteomics 2024;24. https://doi.org/10.1002/pmic.202300135.

[23] Le-Minh V, Tran NT, Makky A, Rosilio V, Taverna M, Smadja C. Capillary zone electrophoresis-native mass spectrometry for the quality control of intact therapeutic monoclonal antibodies. J Chromatogr A 2019;1601:375–84. https://doi.org/10.1016/j.chroma.2019.05.050.

[24] Shen X, Liang Z, Xu T, Yang Z, Wang Q, Chen D, et al. Investigating native capillary zone electrophoresis-mass spectrometry on a high-end quadrupole-time-of-flight mass spectrometer for the characterization of monoclonal antibodies. Int J Mass Spectrom 2021;462:116541. https://doi.org/10.1016/j.ijms.2021.116541.

[25] Gstöttner C, Knaupp A, Vidarsson G, Reusch D, Schlothauer T, Wuhrer M, et al. Affinity capillary electrophoresis – mass spectrometry permits direct binding assessment of IgG and FcγRIIa in a glycoform-resolved manner. Front Immunol 2022;13. https://doi.org/10.3389/fimmu.2022.980291.

[26] Carillo S, Jakes C, Bones J. In-depth analysis of monoclonal antibodies using microfluidic capillary electrophoresis and native mass spectrometry. J Pharm Biomed Anal 2020;185:113218. https://doi.org/10.1016/j.jpba.2020.113218.

[27] Sun Q, Wang L, Li N, Shi L. Characterization and monitoring of charge variants of a recombinant monoclonal antibody using microfluidic capillary electrophoresis-mass spectrometry. Anal Biochem 2021;625:114214. https://doi.org/10.1016/j.ab.2021.114214.

[28] Wu Z, Wang H, Wu J, Huang Y, Zhao X, Nguyen JB, et al. High-sensitivity and high-resolution therapeutic antibody charge variant and impurity characterization by microfluidic native capillary electrophoresis-mass spectrometry. J Pharm Biomed Anal 2023;223:115147. https://doi.org/10.1016/j.jpba.2022.115147.

[29] Füssl F, Trappe A, Carillo S, Jakes C, Bones J. Comparative Elucidation of Cetuximab Heterogeneity on the Intact Protein Level by Cation Exchange Chromatography and Capillary Electrophoresis Coupled to Mass Spectrometry. Anal Chem 2020;92:5431–8. https://doi.org/10.1021/acs.analchem.0c00185.

[30] MacDonald AM, Lucy CA. Highly efficient protein separations in capillary electrophoresis using a supported bilayer/diblock copolymer coating. J Chromatogr A 2006;1130:265–71. https://doi.org/10.1016/j.chroma.2006.05.042.

[31] Schlecht J, Stolz A, Hofmann A, Gerstung L, Neusüß C. nanoCEasy: An Easy, Flexible, and Robust Nanoflow Sheath Liquid Capillary Electrophoresis-Mass Spectrometry Interface Based on 3D Printed Parts. Anal Chem 2021;93:14593–8. https://doi.org/10.1021/acs.analchem.1c03213.

[32] Shen Y, Smith RD. High-resolution capillary isoelectric focusing of proteins using highly hydrophilic-substituted cellulose-coated capillaries. Journal of Microcolumn Separations 2000;12:135–41. https://doi.org/10.1002/(SICI)1520-667X(2000)12:3<135::AID-MCS2>3.0.CO;2-5.

[33] Baek S-J, Park A, Ahn Y-J, Choo J. Baseline correction using asymmetrically reweighted penalized least squares smoothing. Analyst 2015;140:250–7. https://doi.org/10.1039/C4AN01061B.

[34] Niezen LE, Schoenmakers PJ, Pirok BWJ. Critical comparison of background correction algorithms used in chromatography. Anal Chim Acta 2022;1201:339605. https://doi.org/10.1016/j.aca.2022.339605.

[35] Marty MT, Baldwin AJ, Marklund EG, Hochberg GKA, Benesch JLP, Robinson C V. Bayesian Deconvolution of Mass and Ion Mobility Spectra: From Binary Interactions to Polydisperse Ensembles. Anal Chem 2015;87:4370–6. https://doi.org/10.1021/acs.analchem.5b00140.

[36] Hajba L, Guttman A. Recent advances in column coatings for capillary electrophoresis of proteins. TrAC Trends in Analytical Chemistry 2017;90:38–44. https://doi.org/10.1016/j.trac.2017.02.013.

[37] Xu L, Dong X-Y, Sun Y. Novel poly(vinyl alcohol)-based column coating for capillary electrophoresis of proteins. Biochem Eng J 2010;53:137–42. https://doi.org/10.1016/j.bej.2010.10.005.

[38] Alekseychyk L, Su C, Becker GW, Treuheit MJ, Razinkov VI. High-Throughput Screening and Analysis of Charge Variants of Monoclonal Antibodies in Multiple Formulations. SLAS Discovery 2017;22:1044–52. https://doi.org/10.1177/2472555217711666.

[39] Moritz B, Locatelli V, Niess M, Bathke A, Kiessig S, Entler B, et al. Optimization of capillary zone electrophoresis for charge heterogeneity testing of biopharmaceuticals using enhanced method development principles. Electrophoresis 2017;38:3136–46. https://doi.org/10.1002/elps.201700145.

[40] Goyon A, Excoffier M, Janin-Bussat M-C, Bobaly B, Fekete S, Guillarme D, et al. Determination of isoelectric points and relative charge variants of 23 therapeutic monoclonal antibodies. Journal of Chromatography B 2017;1065–1066:119–28. https://doi.org/10.1016/j.jchromb.2017.09.033.

[41] Furey A, Moriarty M, Bane V, Kinsella B, Lehane M. Ion suppression; A critical review on causes, evaluation, prevention and applications. Talanta 2013;115:104–22. https://doi.org/10.1016/j.talanta.2013.03.048.

[42] Lippold S, Nicolardi S, Wuhrer M, Falck D. Proteoform-Resolved FcγRIIIa Binding Assay for Fab Glycosylated Monoclonal Antibodies Achieved by Affinity Chromatography Mass Spectrometry of Fc Moieties. Front Chem 2019;7. https://doi.org/10.3389/fchem.2019.00698.

[43] Dong Q, Liang Y, Yan X, Markey SP, Mirokhin YA, Tchekhovskoi D V., et al. The NISTmAb tryptic peptide spectral library for monoclonal antibody characterization. MAbs 2018;10:354–69. https://doi.org/10.1080/19420862.2018.1436921.

[44] Spanov B, Govorukhina N, Merbel NC van de, Bischoff R. Analytical tools for the characterization of deamidation in monoclonal antibodies. Journal of Chromatography Open 2022;2:100025. https://doi.org/10.1016/j.jcoa.2021.100025.

[45] Turner A, Schiel JE. Qualification of NISTmAb charge heterogeneity control assays. Anal Bioanal Chem 2018;410:2079–93. https://doi.org/10.1007/s00216-017-0816-6.

[46] Shah B, Zhu Y, Wypych J, Zhang Z. Observation of Heavy-Chain C-Terminal Des-GK Truncation in Recombinant and Human Endogenous IgG4. J Pharm Sci 2023;112:1845–9. https://doi.org/10.1016/j.xphs.2023.05.005.

[47] Zhang X, Kwok T, Zhou M, Du M, Li V, Bo T, et al. Imaged capillary isoelectric focusing (icIEF) tandem high resolution mass spectrometry for charged heterogeneity of protein drugs in biopharmaceutical discovery. J Pharm Biomed Anal 2023;224:115178. https://doi.org/10.1016/j.jpba.2022.115178.

[48] Hinterholzer A, Stanojlovic V, Cabrele C, Schubert M. Unambiguous Identification of Pyroglutamate in Full-Length Biopharmaceutical Monoclonal Antibodies by NMR Spectroscopy. Anal Chem 2019;91:14299–305. https://doi.org/10.1021/acs.analchem.9b02513.

[49] Di Marco F, Berger T, Esser-Skala W, Rapp E, Regl C, Huber CG. Simultaneous Monitoring of Monoclonal Antibody Variants by Strong Cation-Exchange Chromatography Hyphenated to Mass Spectrometry to Assess Quality Attributes of Rituximab-Based Biotherapeutics. Int J Mol Sci 2021;22:9072. https://doi.org/10.3390/ijms22169072.

[50] Biacchi M, Gahoual R, Said N, Beck A, Leize-Wagner E, François Y-N. Glycoform Separation and Characterization of Cetuximab Variants by Middle-up Off-Line Capillary Zone Electrophoresis-UV/Electrospray Ionization-MS. Anal Chem 2015;87:6240–50. https://doi.org/10.1021/acs.analchem.5b00928.